Error Propagation in the numerical integration of solitary waves. The regularized long wave equation

A. Araújo * A. Durán †

Abstract

We study the error propagation of time integrators of solitary wave solutions for the regularized long wave equation, $u_t+u_x+\frac{1}{2}(u^2)_x-u_{xxt}=0$, by using a geometric interpretation of these waves as relative equilibria. We show that the error growth is linear for schemes that preserve invariant quantities of the problem and quadratic for 'nonconservative' methods. Numerical experiments are presented.

1 Introduction

The purpose of this paper is to analyze the growth with time of the error of time-integrators for solitary wave solutions of the regularized long wave (RLW) equation; we stablish a better error propagation behaviour for schemes that conserve invariants of the equation. These conservative methods show a linear error growth, while for 'general' integrators, the propagation with time of the error is quadratic. The evolution of these conserved quantities in the numerical integration is also influenced by the conservation properties of the scheme considered.

The advantages of geometric integrators [28], i.e. of methods that mimic geometric properties of the system of differential equations being integrated, are well known [6], [7], [13], [5] in the case of ordinary differential equations; in [14], [11], partial differential equations, as the Korteweg-de Vries equation and the nonlinear Schrödinger equation, have been analyzed. These works are in the origin of the present paper, along with the geometric study given in [10]. We prove that the mechanisms leading to favourable error propagation, that were studied to those equations, can be applied to this case.

*Departamento de Matematica, Universidade de Coimbra, Apartado 3008, 3000 Coimbra, Portugal. E-mail: alma@mat.uc.pt.

†Departamento de Matemática Aplicada y Computación, Universidad de Valladolid, Paseo del Prado de la Magdalena s/n, 47005 Valladolid, Spain. E-mail: angel@mac.cie.uva.es. Correspondence to this author.

Two properties are essential to our results: first, the interpretation of travelling waves as Hamiltonian relative equilibria [1], as in [11], provides a geometric point of view to understand the role of the conserved quantities of the equation in the generation of solitary wave solutions and in the corresponding numerical approximation. On the other hand, in order to investigate the behaviour of these integrators, it is fundamental not only the classical stability analyses [2], [3], [4], [34] for this kind of waves, but also the more recent asymptotic stability results. The papers [26] and [33] were used in [14] and [11] respectively. In this case, asymptotic stability for RLW solitary waves were first observed numerically [12], [22] and the proof of this property is obtained in [21].

The paper is structured as follows: Section 2 presents some relevant properties of the problem being considered, as the Hamiltonian structure of the equation and the existence of solitary wave solutions, arising from a relative equilibrium problem. In Section 3 we analyze the linearization of the equation around one of these solitary wave solutions, while Section 4 is devoted to the main results and to numerical experiments.

A natural extension of this paper concerns the generalization of these techniques to interactions of solitary waves. The equations studied in [14], [11] are examples of integrable partial differential equations: they posses an infinite number of conserved quantities and the so-called soliton property, for which the nonlinear interaction of solitary wave solutions leaves the waves basically unaltered. This is not the case of the RLW equation, that has only a finite number of invariants [24], which indicates that the equation is nonintegrable. The solitary wave interaction problem for the RLW equation has been studied numerically in several papers (see, for example [15], [16], [30], [12]) and, from this point of view, the present work can also be another starting-point in the treatment of this problem.
Some other generalizations of our analysis can be considered. Miller & Weinstein [21] extend their asymptotic stability analysis to the solitary wave solutions of the modified RLW equation, $u_t + u_x + \frac{1}{3}(u^3)_x - u_{xxt} = 0$, and our numerical study could be applied here. On the other hand, the behaviour of higher order terms in the expansion of the error or different discretizations may also be the subject of future work.

2 The regularized long wave equation

2.1 Hamiltonian structure and symmetry groups

The equation treated in the present case is the regularized long wave (RLW) equation

$$u_t + u_x + \frac{1}{2}(u^2)_x - u_{xxt} = 0, \quad -\infty < x < \infty, t > 0. \tag{1}$$

The equation (1) appears in many physical applications [35], [8], [27] and it has been studied extensively. A classical reference is [3]; in fact, (1) is also referred to as the Benjamin-Bona-Mahoney equation. Results on the existence of solutions can also be seen in [21] and numerical works concerning (1) are numerous as well [15], [16], [30], [12], [8]. In the present work, we focus on the Hamiltonian structure of (1). In this case, the phase space Ω for the Hamiltonian formalism consists of sufficiently smooth real functions u of the spatial variable x with its derivatives decreasing sufficiently fast at infinity. Thus, the equation (1) can be expressed as the following infinite-dimensional evolution equation, in Hamiltonian form

$$\frac{du}{dt} = \mathcal{J}\delta H(u), \tag{2}$$

where $\mathcal{J}$ is the skew-adjoint operator [3], [27], [21]

$$\mathcal{J} = -(1-\partial_{xx})^{-1}\partial_x, \tag{3}$$

δ denotes variational derivative and the energy H is given by

$$H(u) = \int_{-\infty}^{\infty} (\frac{1}{2}u^2 + \frac{1}{6}u^3)dx. \tag{4}$$

The Hamiltonian structure associated to the operator (3) is determined by the Poisson bracket [20], [23]

$$\{F, G\} = \int_{-\infty}^{\infty} \delta F \mathcal{J} \delta G dx, \tag{5}$$

Observe that (5) admits Casimir functions [20], [23]; they are functionals with zero Poisson bracket with any other functional. In particular, they give rise to trivial conserved quantities of the equation (1), see [23]. In the subsequent analysis we make use of one of these Casimir functions

$$C(u) = \int_{-\infty}^{\infty} u dx, \tag{6}$$

which we call ‘mass’. The RLW equation also admits another conserved quantity (‘momentum’)

$$I(u) = \int_{-\infty}^{\infty} (\frac{1}{2}u^2 + \frac{1}{2}u_x^2)dx. \tag{7}$$

Observe that $\delta I(u) = (1-\partial_{xx})u$; then the Hamiltonian vector field $v_I = \mathcal{J}\delta I(u) = -u_x$ associated with I, is the infinitesimal generator of the one-parameter symmetry group [23] of the equation (1),

$$G_\epsilon(u(x)) = u(x-\epsilon), \quad \epsilon \in \mathcal{R}, \tag{8}$$

that consists of translations in the spatial variable. This means that G_ϵ is the flow of the vector field v_I. In terms of the Poisson bracket (5), the condition for H to admit the symmetry group (8) is $\{I, H\} = $ constant. In fact, since I is a first integral of (1), we have $\{I, H\} = 0$. The Casimir function (6) is not associated to any other group.

2.2 Solitary wave solutions

The equation (1) admits a two-parameter family of solitary wave solutions [35], [9] that can be seen as relative equilibria [1] associated to the symmetry group (8). The reduction described in [10], [11] can be applied to this case. Here, the phase space Ω is foliated by level sets $\{I = k\}$ of the first integral I. These level sets are manifolds that, because of the involution condition $\{I, H\} = 0$, are invariant by the flow of (1), that is an initial condition on $\{I = k\}$ leads to a solution of (1) remaining on this level set for all t. On the other hand, due to the fact that $\{I, I\} = 0$, each orbit $\{G_\epsilon(u), \epsilon \in \mathcal{R}\}$ of the symmetry group is contained in a level set $\{I = k\}$. Thus, each of these level sets is foliated by orbits of the group and we can construct the corresponding reduced phase space [1], [23], the quotient space consisting of points that are orbits in the original phase space, determined by the value k. On each reduced phase space, the original Hamiltonian system leads to a new Hamiltonian system, the reduced system [1], [23], that governs the time evolution of the group orbits, that is the evolution of u modulo translations in x.

For a fixed level set $\{I = k\}$ we look for relative equilibria $u_0 \in \Omega$ [1]

$$\begin{aligned} \delta H(u_0) - c\delta I(u_0) &= 0, & (9)\\ I(u_0) &= k, & (10) \end{aligned}$$

for, initially, $c \in \mathcal{R}$. We are looking for stationary points of H restricted to the level set. The group orbit through a relative equilibrium u_0 is an equilibrium of the reduced system and the relative equilibrium condition for u_0 generates a solution of (1) from this initial value in a simple way, given by the one-parameter symmetry subgroup: $u(t) = G_{tc}(u_0)$ [10]. Then, the time evolution of the initial profile is given by a translation governed by parameters growing linearly with time.

The substitution of (9) for this case gives

$$cu_0'' - (c-1)u_0 + \frac{1}{2}u_0^2 = 0,$$

generating, for $c > 1$, the solution

$$u_0(x) = 3(c-1)\mathrm{sech}^2\left(\frac{1}{2}\sqrt{1-\frac{1}{c}}x\right). \tag{11}$$

The level set (10) determines the relation with the parameter c:

$$k = \frac{12(c-1)^2}{\sqrt{1-\frac{1}{c}}}\left(1 + \frac{1}{5}\left(1-\frac{1}{c}\right)\right).$$

The group orbit through u_0 gives rise to a one-parameter family of solutions

$$\varphi(x, x_0) = G_{x_0}(u_0) = u_0(x - x_0). \tag{12}$$

Every solution (12) projects onto the same equilibrium in the reduced phase space. Finally, we obtain the solutions of (1) given by

$$\psi(x,t,c,x_0) = G_{tc}(\varphi) = 3(c-1)\mathrm{sech}^2(\frac{1}{2}\sqrt{1-\frac{1}{c}}(x-ct-x_0)). \qquad (13)$$

This is a two-parameter family of solitary wave solutions. The parameter c determines not only the velocity of the wave but also its amplitude (compare with [14], [11]), with the taller the wave the faster it travels. On the other hand, x_0 governs the initial location.

3 The variational equation

3.1 The homogeneous linearized equation

The time propagation of the error in the numerical integration of solitary wave problems for (1) can be studied by analyzing the solutions of the corresponding linearized equation of (1) near a relative equilibrium solution like ψ in (13). If δ denotes the perturbation of ψ from an initial small change $\psi(x,0,c,x_0)+\epsilon\delta_0(x)$, then δ satisfies the homogeneous variational equation

$$(1-\partial_{xx})\delta_t + \partial_x(\delta+\psi\delta) = 0. \qquad (14)$$

With the change of variables given by the symmetry group $\delta = G_{tc}\Delta$ [11] we can write (14) as

$$\Delta_T - \Delta_{\xi\xi T} + c\Delta_{\xi\xi\xi} + \partial_\xi((1-c)\Delta + \psi\Delta) = 0, \qquad (15)$$

with $\xi = x-ct-x_0$, $T=t$. Now, (15) can be expressed as an evolution equation

$$\Delta_T = L\Delta, \qquad (16)$$

with the operator L given by [21]

$$\begin{aligned} L &= (1-\partial_{\xi\xi})^{-1}\partial_\xi L_c, &(17)\\ L_c &= -c\partial_{\xi\xi} + c - 1 - \psi(\xi). &(18) \end{aligned}$$

As in [11] we will also treat with the corresponding nonhomogeneous variational equation for source terms that admit $\{G_{tc} : t \in \mathcal{R}\}$ as a symmetry group. By using the change of variables above, we can present this nonhomogeneous case as

$$\Delta_T = L\Delta + s, \qquad (19)$$

with s constant.

In order to study (16) in more detail, we consider the Sobolev space H_a^1 [26], [21] that consists of functions $v(\xi)$ such that $e^{a\xi}v(\xi) \in H^1(\mathcal{R})$, for a constant a with $0 < a < \sqrt{1-\frac{1}{c}}$. The norm considered is

$$||v||_{H_a^1} = ||e^{a\xi}v||_{H^1}.$$

Observe that the solitary wave $\psi(\xi)$ and its derivatives belong to this space.

The spectral properties of the operator L are analyzed in [21]:

Lemma 3.1 *There exists $c^* > 1$ such that for all $c \in (1, c^*]$ and for all but a discrete set of $c \geq c^*$, $\lambda = 0$ is the only eigenvalue of L in H_a^1 with* $\mathrm{Re}\lambda \geq 0$, *where $0 < a < \sqrt{1-\frac{1}{c}}$. The geometric multiplicity of this eigenvalue is* 1 *and the algebraic multiplicity is* 2. *The generalized kernel of L,* $\mathrm{Ker}_g L$, *is spanned by the functions*

$$\Phi_1(\xi) = \frac{\partial \psi}{\partial x_0}, \tag{20}$$

$$\Phi_2(\xi) = \frac{\partial \psi}{\partial c}, \tag{21}$$

with $L\Phi_1 = 0$, $L\Phi_2 = \Phi_1$.

Then, (16) has solutions of the form

$$\alpha\Phi_1 + \beta(\Phi_2 + T\Phi_1),$$

which, in terms of the original variables x, t, are linear combinations of the partial derivatives of the solitary wave with respect to x_0 and c. They represent changes of the solitary wave due to the perturbation of its parameters. Explicitly, Φ_1 corresponds to the group generator v_I at the solitary wave and therefore induces changes in the location x_0 of the wave. On the other hand, Φ_2 is associated to modifications in the solitary wave corresponding to changes in the value of I, determined by c.

We denote by P the projection of H_a^1 onto the generalized kernel of L and by Q its complement $I - P$, that is

$$\begin{aligned} Pv &= \langle v, \Psi_1\rangle\Phi_1 + \langle v, \Psi_2\rangle\Phi_2, \\ Qv &= v - Pv. \end{aligned} \tag{22}$$

Here, Ψ_1 and Ψ_2 form a basis of the generalized kernel of the adjoint operator L^* of L, where $\langle\cdot,\cdot\rangle$ denotes the L^2 inner product. These functions can be chosen in such a way that $\langle\Phi_i, \Psi_j\rangle = \delta_{ij}$. More precisely [21]

$$\begin{aligned} \Psi_1 &= \theta_1(\partial_\xi\Phi_2 - \int_{-\infty}^{\xi}\Phi_2(y)dy) + \theta_2(1-\partial_{\xi\xi})\psi, \\ \Psi_2 &= \theta_3(1-\partial_{\xi\xi})\psi, \end{aligned} \tag{23}$$

where

$$\theta_1 = \frac{-1}{\frac{d}{dc}I(\psi)}, \quad \theta_2 = \frac{-1}{2}\Big(\frac{\frac{d}{dc}C(\psi)}{\frac{d}{dc}I(\psi)}\Big)^2, \quad \theta_3 = \theta_1.$$

In fact, $L^*\Psi_2 = 0$ and $L^*\Psi_1 = -\Psi_2$. Observe that Ψ_2 is essentially the gradient of the invariant I evaluated at the solitary wave ψ.

An important result to analyze the solutions of the nonhomogeneous version (19) is also due to Miller & Weinstein [21]. They show that the operator L generates a C_0 semigroup with exponentially decaying H^1_a norm on the spectral complement of its generalized kernel.

Lemma 3.2 *Assume that $0 < a < \sqrt{1-\frac{1}{c}}$ and that $\lambda = 0$ is the only eigenvalue of L in H^1_a with $\mathrm{Re}\lambda \geq 0$. Let Q denote the projection onto $\mathrm{Ker}_g(L^*)^\perp$ (see (22)). If $\Delta(T)$ is a solution of (16) with initial condition $\Delta_0 \in H^1_a \bigcap Q(H^1_a)$, then $\Delta(T) \in H^1_a \bigcap Q(H^1_a)$ for all T and there are constants $k_1, k_2 > 0$ such that*

$$||\Delta(T)||_{H^1_a} \leq k_1 e^{-k_2 T}||\Delta_0||_{H^1_a}. \tag{24}$$

That is, solutions of (16) with initial data in $X = H^1_a \bigcap \mathrm{Ker}_g(L^*)^\perp$ decay exponentially to zero in H^1_a norm as $t \to \infty$. As far as the H^1 norm is concerned, observe that solutions of (16) conserve the functional

$$F(\Delta) = \int_{-\infty}^{\infty} \big(\frac{c}{2}(\partial_\xi \Delta)^2 + \frac{(c-1)}{2}\Delta^2 - \frac{1}{2}\psi\Delta^2\big)d\xi,$$

(recall that $c > 1$); therefore, if $\Delta(T)$ is a solution of (16), we have

$$\begin{aligned}
||\Delta(T)||^2_{H^1} &\leq \frac{2}{c-1}F(\Delta(T)) + \frac{1}{c-1}\int_{-\infty}^{\infty}\psi\Delta^2 d\xi \\
&= \frac{2}{c-1}F(\Delta_0) + \frac{1}{c-1}\int_{-\infty}^{\infty}\psi e^{-2a\xi}\Delta^2 e^{2a\xi}d\xi \\
&\leq \frac{2}{c-1}F(\Delta_0) + C||\Delta(T)||_{H^1_a}||\Delta(T)||_{H^1} \\
&\leq \frac{2}{c-1}F(\Delta_0) + \frac{1}{2}||\Delta(T)||^2_{H^1} + C'||\Delta(T)||^2_{H^1_a}.
\end{aligned}$$

Now, $F(\Delta_0)$ can be written in terms of $||\Delta_0||_{H^1}$ and we have the following estimate:

Lemma 3.3 *Under the conditions of Lemma 3.2, if $\Delta_0 \in X \bigcap H^1$, then there exists $k_1, k_2 > 0$ such that*

$$||\Delta(T)||_{H^1} \leq k_1(||\Delta_0||_{H^1} + e^{-k_2 T}||\Delta_0||_{H^1_a}). \tag{25}$$

Observe that, since the symmetry group (8) consists of translations, the growth with time of solutions of (14) is similar to that of solutions of (16). The estimate (25) implies that the only source of growth with time of these solutions comes from its component in the generalized kernel of L, that is the term that represents perturbations in the parameters of the solitary wave.

3.2 The nonhomogeneous variational equation

The results above are essential to study the solutions of (18). If $s = s(\xi) \in H^1_a$, we can decompose $s = s_P + s_Q$ with $s_P \in \mathrm{Ker}_g L$, $s_Q = Qs \in X$. By using Lemma 3.1, we can write $s_P = s_1 + s_2$ for $s_1 \in \mathrm{Ker} L$ and s_2 in a supplement of $\mathrm{Ker} L$ in $\mathrm{Ker}_g L$. More precisely,

$$s_1 = \alpha_1 \Phi_1, \quad s_2 = \alpha_2 \Phi_2,$$

with

$$\alpha_i = \langle s, \Psi_i \rangle, \qquad i = 1, 2. \tag{26}$$

In this context, we have

Lemma 3.4 *If $0 < a < \sqrt{1 - \frac{1}{c}}$ and $s \in H^1_a$, the solution of (19) with zero initial condition can be written in the following way:*

$$\Delta(T) = \alpha_1 T \Phi_1 + \alpha_2 (T \Phi_2 + \frac{T^2}{2} \Phi_1) + \Gamma(T), \tag{27}$$

where α_1, α_2 are given by (26). The function Γ is of the form

$$\Gamma(T) = \int_0^T \exp((T - \tau)L) s_Q d\tau. \tag{28}$$

Moreover, if $s_Q \in H^1$ and there exists $\beta \in H^1 \bigcap H^1_a$ such that $s_Q = L\beta$, then $\Gamma(T)$ remains, for all T, bounded in the H^1 norm.

Proof. The expression (27) can be proved by using Duhamel's principle and the previous results in a similar way to that of [11]. Observe that we can write

$$\Delta(T) = T s_1 + (TI + \frac{T^2}{2} L) s_2 + \int_0^T \exp((T - \tau)L) s_Q d\tau,$$

where I is the identity operator. The substitution of s_1 and s_2 proves the first part of the Lemma. Note that the estimate (25) shows that, if $s_Q \in H^1$, then $\Gamma(T)$, with a bounded integrand, grows at most linearly with time in the H^1 norm. On the other hand, if Qs is in the range of the operator L, $Qs = L\beta$ for $\beta \in H^1 \bigcap X$ ($Q(H^1_a)$ is invariant by L), then we can write $\Gamma(T)$ in the form

$$\Gamma(T) = (\exp(TL) - I)\beta,$$

and we use Lemma 3.3 to conclude the proof. □

Remarks

(a) Note that the first two terms in (27) correspond to the projection of the solution on $\mathrm{Ker}_g L$, with its components in $\mathrm{Ker}L$ (Ts_1 and $\frac{T^2}{2}Ls_2$) lying in the direction of the group generator at the solitary wave solution. The component in $\mathrm{Ker}_g L$ but not in $\mathrm{Ker}L$ corresponds to the variation of the relative equilibrium with respect to the parameter c, that governs the level manifold. Then, this first part represents perturbations in the wave parameters, growing quadratically with time in the direction of $\mathrm{Ker}L$ (in the group parameter x_0) and linearly in the level set parameter c. If the source term s is orthogonal to the gradient of I evaluated at the solitary wave, then $s_2 = 0$ and the growth is linear.

(b) The behaviour of the integral $\Gamma(T)$ in (28) shows that the perturbations that do not correspond to changes in wave parameters grow at most linearly with time in the H^1 norm. In the following Section, we deal with smooth source terms $s = s(\xi)$ in $H^1 \bigcap H^1_a$ which are orthogonal to the gradients of the invariants C and I at the solitary wave. In this case, these perturbations can be controlled in H^1 norm uniformly in time. To see this, we first observe that the orthogonality conditions imply

$$\langle s, 1\rangle = \langle s, \Psi_2\rangle = 0,$$

with Ψ_2 given by (23). Therefore,

$$\begin{aligned}\langle Qs, 1\rangle &= \langle s, 1\rangle - \langle s, \Psi_1\rangle\langle \Phi_1, 1\rangle - \langle s, \Psi_2\rangle\langle \Phi_2, 1\rangle \\ &= \langle s, \Psi_1\rangle\langle \Phi_1, 1\rangle = 0,\end{aligned}$$

(the last expression vanishes because $\langle \Phi_1, 1\rangle = 0$). Then we can define

$$F(\xi) = \int_{-\infty}^{\xi} Qs(y)dy,$$

that is a smooth function in $H^1 \bigcap H^1_a$ such that $\partial_\xi F = Qs$. On the other hand, the operator L can be written as

$$L = \partial_\xi M_c, \qquad M_c = (1 - \partial_{\xi\xi})^{-1} L_c,$$

and the operator L_c, given by (18), is selfadjoint in L^2 with $\mathrm{Ker}L_c = \mathrm{span}(\partial_\xi \psi)$ [33]. Now, we have

$$\langle (1 - \partial_{\xi\xi})F, \partial_\xi \psi\rangle = -\langle \partial_\xi F, (1 - \partial_{\xi\xi})\psi\rangle = -\frac{1}{\theta_2}\langle Qs, \Psi_2\rangle = 0.$$

This means that F is in the range of M_c; therefore Qs is in the range of L and the last part of Lemma 3.4 applies.

4 Numerical approximation

4.1 Main results

We make use of the preceding theoretical results in order to study the behaviour in time of approximations to a solitary wave of the family (13). We consider a semidiscrete (discrete t, continuous x) one-step integrators for the initial value problem for (1) of the form

$$U^{n+1} = \chi_{\Delta t}(U^n), \tag{29}$$

where Δt denotes the time step, $U^n = U^n(x)$ is a numerical solution at time level $t_n = n\Delta t, n = 0, 1, \ldots$ and $\chi_{\Delta t}$ approximates the flow of the equation. Thus, if $U^0 = u_0$, then U^n is an approximation to the value $u(t_n)$ of the solution u of (1) with initial condition u_0.

We make some additional hypotheses about the method (29). Taking u_0 as the relative equilibrium φ like (12) and if the corresponding solution ψ in (13) is approximated by (29) with $U^0 = \varphi$, we first assume that the local error at ψ, that is the difference between the true Δt-flow at ψ and $\chi_{\Delta t}(\psi)$, admits an expansion of the form

$$\Delta t^{r+1} l(\psi) + \Delta t^{r+1} R(\psi, \Delta t), \tag{30}$$

where r is the order of the method, l, R are mappings defined in Ω with values in Ω, l is independent of Δt and $||R(\cdot, \Delta t)||_{H^1} \to 0$ as $\Delta t \to 0$. It is also reasonable to suppose that $l = l(\psi)$ is a smooth function in $H^1 \bigcap H_a^1$, since this mapping depends on ψ and its derivatives, which belong to this space [14].
The second hypothesis states the invariance of the mapping $\chi_{\Delta t}$ by the one-parameter group $\{G_{tc} : t \in \mathcal{R}\}$ so that the mapping l in (30) admits this group as a symmetry group. Note that, since the group consists of translations and most standard integrators are invariant with respect to linear transformations [31], this condition is not restrictive.
Finally, we also assume that the global error $U^n(x) - \psi(x, t_n)$ has an asymptotic expansion of the form

$$U^n(x) - \psi(x, t_n) = \Delta t^r e(x, t_n) + \Delta t^r q(x, t_n, \Delta t), \quad -\infty < x < \infty, \tag{31}$$

where the function e is independent of Δt and satisfies the corresponding nonhomogeneous variational equation [7]

$$\begin{aligned} (1 - \partial_{xx})e_t + \partial_x(e + \psi e) &= -l(\psi), \quad -\infty < x < \infty, t > 0, \\ e(x, 0) &= 0. \end{aligned}$$

Moreover, q is a remainder that, for fixed t, tends to zero in the H^1 norm as $\Delta t \to 0$.

The following theorem describes the asymptotic behaviour with time of the approximation to the solitary wave, given by (29).

Theorem 4.1 *(i) (General case). Assume that (30), (31) hold and* $\chi_{\Delta t}$ *is invariant by the one-parameter group* $\{G_{tc} : t \in \mathcal{R}\}$*. Then, we have*

$$U^n(x) = \psi(x, t_n, \tilde{c}, \tilde{x_0}) + \Delta t^r \rho(x, t_n) + \Delta t^r Q(x, t_n, \Delta t), \qquad (32)$$

where

$$\begin{aligned} \tilde{c} &= c + \alpha_2 t_n \Delta t^r, & (33) \\ \tilde{x_0} &= x_0 + (\alpha_1 t_n + \alpha_2 \frac{t_n^2}{2}) \Delta t^r, & (34) \end{aligned}$$

with $\alpha_i = -\langle l, \Psi_i \rangle, i = 1, 2$*. The function* ρ *is independent of* Δt *and there is a constant* $C > 0$ *such that* $||\rho(\cdot, t)||_{H^1} \leq Ct$*. The function* Q *is a remainder such that, for fixed* t*,* $||Q(\cdot, t, \Delta t)||_{H^1} \to 0$ *as* $\Delta t \to 0$*.*

(ii) (Conservative case). If the method (29) satisfies

$$\langle l, \delta I(\varphi) \rangle = 0, \qquad (35)$$

then (34) holds with $\alpha_2 = 0$*. Moreover, if*

$$\langle l, 1 \rangle = 0, \qquad (36)$$

then the function ρ *is bounded in the* H^1 *norm uniformly in time.*

Proof. The proof of (i) is similar to that of [11]. Observe that the term ρ corresponds to the component of the function e that lies in the spectral complement of the generalized kernel of L [27]. By using Lemmas 3.3 and 3.4 this term grows, in general, at most linearly in time. On the other hand, if the method satisfies (35), since Ψ_2 is, except multiplicative constant, the gradient of the invariant at the solitary wave (see (23)), then it is clear that $\alpha_2 = 0$.
It is remain to show the last part of (ii). But if (35), (36) hold, then Remark (b) of Subsection 3.2 applies and the function ρ is bounded in the H^1 norm. □

From the expansion (32) we note that the so-called *modified solitary wave* [14], [11], that is the first term of the right hand side of (32) has a new velocity $\tilde{c}$, given by (33) (and therefore a new amplitude) that is a linear with time perturbation of the velocity c of the original wave, while the new location $\tilde{x_0}$, given by (34), differs from the original x_0 in terms that grow quadratically with time. If the method conserves the quantity I, then [14] it satisfies (35) and the modified wave keeps the original velocity (and therefore amplitude) while the perturbation of x_0 that determines the modified location $\tilde{x_0}$ reduces its growth with time, being only linear. Note that the same conclusion can be reached if the method preserves the Hamiltonian (4) instead of I. In this case, the leading term of the local error is orthogonal to the gradient of H at the solitary wave; but the relative equilibrium condition (9) of this wave implies that this gradient is proportional to the gradient of I at this wave and, therefore, the scheme also satisfies (35).

We can also note that, if the method conserves the Casimir function C, then (36) holds. But, since C is a linear functional, it is preserved by practically all methods used in practice [18], so (36) is not an exigent condition.

The second term $\Delta t^r \rho$ of the right hand side of (32) is a *complementary term [14], [11]* that represents errors of leading order $O(\Delta t^r)$ not associated to changes in the parameters of the wave. Recall that it corresponds to the component of the leading term of the global error in X. In the 'conservative' case, this term is bounded in the H^1 norm, being necessary to impose the conservation not only of the quantity I but also of the Casimir C in order to obtain this bounded behaviour. Note that the invariant C does not seem to play any role in the perturbation of the parameters of the solitary wave solution, see (33), (34), while we can see the influence of the invariant I in both the modified wave and the complementary term.
Finally, the third term in (32) $\Delta t^r Q$ is a remainder of higher order $o(\Delta t^r)$.

4.2 Numerical experiments

The purpose of the experiments below is to show some advantages of the use of numerical schemes that conserve some invariant in the numerical integration of the solitary wave problem for the RLW equation (1), rather than to compare the efficiency of the methods. This idea will influence not only in the type of experiments being presented, but also in the choice of the integrators being used.

- From this point of view, we first consider the well known implicit midpoint rule, which we call [ICM]. This method has order two and conserves quadratic invariants of the system being integrated [29]. In our case, it preserves the quantity I but not the Hamiltonian (4).

- We can interchange the invariant to be preserved and construct a second-order method [HCM] that conserves the Hamiltonian but not the functional I [32], [19]. This scheme can be written as

$$\begin{aligned} U^{n+1} &= U^n - \Delta t(1-\partial_{xx})^{-1}\partial_x(U^{n+1/2} + G(U^n, U^{n+1})), \\ U^{n+1/2} &= \frac{U^n + U^{n+1}}{2}, \\ G(U^n, U^{n+1}) &= \frac{F(U^{n+1}) - F(U^n)}{U^{n+1} - U^n}, \quad F(U) = \frac{1}{6}U^3. \end{aligned}$$

- Finally, the Simply Diagonally Implicit Runge-Kutta method [NCM],

$$\begin{array}{c|cc} & \gamma & 0 \\ & 1-2\gamma & \gamma \\ \hline & 1/2 & 1/2 \end{array}$$

with $\gamma = (3+\sqrt{3})/6$ and order three (see [17]), has been chosen to illustrate the behaviour of a typical nonconservative scheme, because this method does not preserve any of the quantities I, H.

It is not difficult to prove that the three methods considered conserve the Casimir function C. In fact, we have preferred to use methods with some degree of competitivity instead of to construct mass nonpreserving integrators.

We present results concerning approximations to the solitary wave (13) with parameters $c = 2$ (amplitude 3) and initial location $x_0 = -10$. To implement the methods, we use a fully aliased pseudospectral spatial discretization in such a way that, virtually, errors obtained correspond only to the time discretization [14]. We succesively refined the spatial grid until one was found for which no further error reduction was possible. On the other hand, standard analyses can check the validity of the hypotheses of the Theorem 4.1 for the three integrators considered [11]. We classify the numerical experiments presented in three classes:

- Differences in long time behaviour of the approximations in connection with conservation properties.
- Differences between the elements of the solitary wave solution and the form of the corresponding numerical approximation.
- Differences in time behaviour of the invariants I and H through numerical integration.

We first study the propagation in time of the global error of each method. Figure 1 shows the L^2 norm of the error as a function of time, in log-log scale, up to $t_{\max} = 200$. Here, the solid lines correspond to [ICM] and the dashed lines to [NCM]. Figure 2 only differs from Figure 1 in the scheme associated to the solid lines, that now represent [HCM]. The step sizes (for the two figures) are $\Delta t = 1/20, 1/40, 1/80, 1/160$.
The results of Table 1, which gives the errors at the final time $t_{\max} = 200$ for the three methods, show the order of convergence, $r = 2$ for [ICM] and [HCM] and $r = 3$ for [NCM]. This can also be observed in Figures 1 and 2 by watching the distance between parallel lines corresponding to a given method. On the other hand, the slopes of the lines show that, for [ICM] and [HCM], errors grow linearly with time, while for [NCM] the growth is quadratic (compare with the lines plotted in the right down corner of the figures). Recall that the second-order methods [ICM] and [HCM] conserve, respectively, the momentum I and the Hamiltonian H; according to Theorem 4.1, the parameters of the solitary wave solution are perturbed in terms that grow at most linearly with time. The behaviour in error propagation must be different in the case of [NCM], that does not preserve any of the quantities and, in fact, the leading term of its local error

does not satisfy (35); here, the perturbations of the parameters grow quadratically with time.

From Figures 1 and 2 we can also observe that, for some values of the time step Δt, [ICM] and [HCM] give smaller errors at the final time $t_{\max} = 200$ than the third order scheme [NCM] (see, for example, the lines corresponding to $\Delta t = 1/20, 1/40$). The different behaviour with time of the error propagation suggests that, for long time integrations, it seems to be advisible to use an integrator with some conservation property.

The conservative character of a scheme influences not only in the perturbations of the parameters of the wave (and therefore in the construction of the corresponding modified solitary wave) but also in the behaviour in time of the complementary term (see Theorem 4.1). This can be analyzed numerically, for moderate values of t, by computing the parameters of the modified solitary wave $\tilde{c}$ and $\tilde{x_0}$, and by measuring the errors between this new wave and the corresponding numerical solution. Table 2 gives these modified errors, in L^2 norm, for the three schemes, at the final time $t_{\max} = 200$. Observe that in all cases, the modified error for any of the values of Δt considered is smaller than the corresponding true error (compare with Table 1). Most of the error is incorporated to the perturbations of the parameters that determined the modified solitary wave. Figures 3 and 4 illustrate the evolution in time of the modified error for [HCM] and [NCM] respectively (the case of [ICM] is similar to that of [HCM] and it provides no further information). Recall that the theoretical results reveal that, in the conservative case, the complementary term is bounded in time, while in the general case, the growth of this element is at most linear with t. This different behaviour is shown in Figure 3, reflecting the bounded behaviour in the conservative case, and in Figure 4, where error grows linearly with time.

Note that, since we only analyze the evolution in time of the leading term of the global error, not many things can be said about the remainder, whose behaviour in time should also influence in some way. At this point, two facts can be remarked. First, from Table 2 we see that, in the case of the second-order methods [ICM] and [HCM], modified errors behave as $O(\Delta t^2)$ suggesting that, for the values of Δt considered, the complementary term dominates over the remainder; however the influence of the remainder is noted in the case of [NCM], where modified errors do not have an $O(\Delta t^3)$ behaviour for moderate values of Δt relative to the final time of integration (see the values of the modified error corresponding to [MCN] for $\Delta t = 1/10, 1/20, 1/40$, in Table 2). When we have smaller values of the time step, the complementary term becomes dominant. This seems to show that, for a long final time $t_{\max}$, we need smaller Δt to find the leading order of the method in the modified errors.

On the other hand, by making the final time of integration longer and by retaining a fixed Δt, we have observed that the bounded behaviour of the complementary term, in the conservative case of [ICM] and [HCM], is lost, being substituted by the growth of terms hidden in the remainder. Here we conclude the first type of numerical experiments.

The structure of the numerical solution can be nicely illustrated by plotting the solitary waves. Here, other differences are noted. Figure 5 shows, at $t = 100$, the true solitary wave, with solid line, while the broken line and the crosses represent, respectively, the modified solitary wave and the numerical solution corresponding to [HCM], with $\Delta t = 1/20$. Figure 6 displays the same elements for the case of [NCM]. In both cases, we see that the numerical solution essentially behaves as a solitary wave, closer to the corresponding modified wave than to the solution (see Tables 1 and 2). For the 'conservative' scheme [HCM], the modified wave differs from the original one in a linear in time perturbation in the initial location (see Theorem 4.1) which in the case of the figure delays its motion with respect to that of the true wave. However, the modified wave keeps the original velocity, and therefore amplitude. Hence, the modified wave associated to [HCM] also preserves the value of the 'mass' of the original solitary wave, represented by the Casimir function C

$$C(\psi) = 12\sqrt{c(c-1)},$$

because this quantity only depends on the velocity c.

This is not the situation in the case of the 'nonconservative' method [NCM]. Here, the modified wave has a different velocity of propagation and therefore amplitude, see (33), growing linearly with time with respect to the velocity of the solution. This is visible in Figure 6. In particular, the modified wave does not conserve the 'mass' C. Since the numerical solution is mass conserving, the mass lost in the approximation to the modified solitary wave is recovered in the formation of a tail [14] behind the numerical solitary wave profile. This tail can be observed in Figure 7, which displays the numerical solution appearing in Figure 6, but with a vertical scale with some more degrees of magnitude. This phenomenum does not occur in the conservative case.

Finally, we complete the numerical experiments by analyzing the behaviour, through the numerical integration, of the conserved quantities I and H. We study the evolution of the differences

$$H(U^n) - H(\psi(t_n)) = H(U^n) - H(U^0), \tag{37}$$

$$I(U^n) - I(\psi(t_n)) = I(U^n) - I(U^0), \tag{38}$$

between the values of I and H at the solitary wave solution and the discrete versions of the quantities, at the numerical solution given by [HCM], for (38), and by [NCM], for both (37) and (38). These discrete versions of the invariants use the pseudospectral space discretization and are good approximations of the quantities at the corresponding semidiscrete numerical solution [25]. Observe that, since I and H are conserved quantities of the problem, the differences (37) and (38) also estimate the evolution of I and H in the numerical integration. Figures 8 and 9 represent, respectively, the evolution of I and H at the numerical solution given by [NCM], while Figure 10 shows the values (38) in the case of [HCM].

Recall that, in general, the difference between an invariant of the problem considered at the numerical approximation and at the true solution is of the order of the method [14]; if we expand this difference in powers of Δt, the coefficient of the leading term is the inner product between the gradient of the invariant at the true solution and the leading term of the asymptotic expansion of the global error. This dominant order can be seen, in the case of [NCM], in Figures 8 and 9, where errors (37) and (38) show an $O(\Delta t^3)$ behaviour. However, as far as [HCM] is concerned, note that, the leading term of its local error is orthogonal not only to the gradient of H at ψ (because the scheme is Hamiltonian conserving) but also to the gradient of the other quantity I at the solitary wave (because of the relative equilibrium condition (9)). This fact and the conservation of I by the solution ψ implies [14], [11] that the leading term of the global error is also orthogonal to that gradient; then as $\Delta t \to 0$ with t_n fixed, the order of the error (38) is $o(\Delta t^2)$. Figure 10 shows an $O(\Delta t^4)$ behaviour.

Acknowledgements.

This research has been supported by the Center of Mathematics, Universidade de Coimbra. A.D. is very grateful for the hospitality of the Department of Mathematics of this university, where this work was done.

References

[1] V.I. Arnold, *Mathematical Methods of Classical Mechanics*, Springer-Verlag, Berlin, 1989.

[2] T.B. Benjamin, *The stability of solitary waves*, Proc.Roy.Soc.London Ser. A 328 (1972), 153-183.

[3] T.B. Benjamin, J.L. Bona & J.J. Mahoney, *Model equations for long waves in nonlinear dispersive systems*, Philos. Trans. Roy. Soc. London Ser. A 272 (1972), 47-78.

[4] J.L. Bona & A. Soyeur, *On the stability of solitary wave solutions of model equations for long waves*, J. Nonlinear Sci. 4(1994), 449-470.

[5] M.P. Calvo & E. Hairer, *Accurate long-term integration of dynamical systems*, Appl. Numer. Math. 18(1995), 95-105.

[6] M.P. Calvo & J.M. Sanz-Serna, *The development of variable-step symplectic integrators with application to the two-body problem*, SIAM J. Sci. Comput. 14(1993), 936-952.

[7] B. Cano & J.M. Sanz-Serna, *Error growth in the numerical integration of periodic orbits, with application to Hamiltonian and reversible systems*, SIAM J. Numer. Anal. 34(1997), 1391-1417.

[8] W. Craig & M. Groves, *Hamiltonian long-wave approximations to the water-wave problem*, Wave Motion 19(1994),367-389.

[9] P.G. Drazin & R.S. Johnson, *Solitons. An Introduction*, Cambridge Texts in Applied Mathematics, Cambridge University Press, Cambridge, 1990.

[10] A. Durán & J.M. Sanz-Serna, *The numerical integration of relative equilibrium solutions. Geometric theory*, Nonlinearity 11(1998), 1547-1567.

[11] A. Durán & J.M. Sanz-Serna, *The numerical integration of relative equilibrium solutions. The nonlinear Schrödinger equation*, to appear in IMA J. Numer. Anal.

[12] J.C. Eilbeck & G.R. McGuire, *Numerical study of the regularized long-wave equation II: interaction of solitary waves*, J. Comput. Phys. 23(1977), 63-73.

[13] D.J. Estep & A. M. Stuart, *The rate of error growth in Hamiltonian conserving integrators*, Z. Angew. Math. Phys. 46(1995), 407-418.

[14] J. de Frutos & J.M. Sanz-Serna, *Accuracy and conservation properties in numerical integration: the case of the Korteweg-de Vries equation*, Numer. Math. 75(1997), 421-445.

[15] L.R.T. Gardner & G.A. Gardner, *Solitary waves of the regularised long-wave equation*, J. Comput. Phys. 91(1990), 441-459.

[16] L.R.T. Gardner & G.A. Gardner, *Solitary waves of the equal width wave equation*, J. Comput. Phys. 101(1992), 218-223.

[17] E. Hairer, S.P. Nørsett & G. Wanner, *Solving Ordinary Differential Equations I, Nonstiff Problems*, 2nd edn, Springer-Verlag, Berlin, 1993.

[18] C.W. Gear, *Invariants and numerical methods for ODEs*, Physica D, 60 (1990), 303-310.

[19] T. Itoh & K. Abe, *Hamiltonian-conserving discrete canonical equations based on variational difference quotients*, J. Comput. Phys. 77(1988), 85-102.

[20] J.E. Marsden & T.S. Ratiu, *Introduction to Mechanics and Symmetry*, Springer-Verlag, New York, 1994.

[21] J.R. Miller & M.I. Weinstein, *Asymptotic stability of solitary waves for the regularized long-wave equation*, Comm. Pure Appl. Math. 49(1996), 399-441.

[22] P.J. Morrison, J.D. Meiss & J.R. Cary, *Scattering of regularized-long-wave solitary waves*, Phys. D 11(1984),324-336.

[23] P.J. Olver, *Applications of Lie Groups to Differential Equations*, 2nd edn, Springer-Verlag, New York, 1993.

[24] P.J. Olver, *Euler operators and conservation laws of the BBM equation*, Math. Proc. Cambridge Philos. Soc., 85(1979), 143-160.

[25] D. Pathria & J.L Morris, *Pseudospectral solution of nonlinear Schrödinger equations*, J. Comput. Phys. 87(1990), 108-125.

[26] R. Pego & M.I. Weinstein, *Asymptotic stability of solitary waves*, Comm. Math. Phys. 164(1994), 305-349.

[27] D.H. Peregrine, *Calculations of the development of an undular bore*, J. Fluid Mech., 25(1996), 321-330.

[28] J.M. Sanz-Serna, *Geometric integration*, in The State of the Art in Numerical Analysis, I.S. Duff & G.A. Watson eds., Clarendon Press, Oxford, 1997, 121-143.

[29] J.M. Sanz-Serna & M.P. Calvo, *Numerical Hamiltonian Problems*, Chapman & Hall, London, 1994.

[30] D.M. Sloan, *Fourier pseudospectral solution of the regularised long wave equation*, J. Comput. Appl. Math. 36(1991), 159-179.

[31] D. Stoffer, *Variable steps for reversible integration methods*, Computing, 55(1995), 1-22.

[32] W.A. Strauss & l. Vázquez, *Numerical solution of a nonlinear Klein-Gordon equation*, J. Comput. Phys. 28(1978),271-278.

[33] M.I. Weinstein, *Modulational stability of ground states of nonlinear Schrödinger equations*, SIAM J. Math. Anal. 16(1985), 473-491.

[34] M.I. Weinstein, *Existence and dynamic stability of solitary wave solutions of equations arising in long wave propagation*, Comm. Partial Differential Equations 12(1987), 1133-1175.

[35] G.B. Whitham, *Linear and Nonlinear Waves*, J. Willey & Sons, New York, 1974.

Table 1: Errors with respect to the solitary wave at $t = 200$.

Δt	ICM	HCM	NCM
1E-01	6.5680E-01	5.7426E-01	–
5E-02	1.6527E-01	1.4447E-01	3.9329E-01
2.5E-02	4.1371E-02	3.6164E-02	4.9593E-02
1.25E-02	1.0346E-02	9.0438E-03	6.2069E-03
6.25E-03	2.5866E-03	2.2611E-03	7.7595E-04
3.125E-03	6.4667E-04	5.6530E-04	9.6989E-05

Table 2: Errors with respect to the modified solitary wave at $t = 200$.

Δt	ICM	HCM	NCM
1E-01	8.1552E-02	3.8517E-02	1.4539E-01
5E-02	1.9753E-02	9.0863E-03	3.6307E-03
2.5E-02	4.8981E-03	2.2376E-03	2.5108E-04
1.25E-02	1.2220E-03	5.5732E-04	3.1149E-05
6.25E-03	3.0538E-04	1.3918E-04	3.9005E-06
3.125E-03	7.6328E-05	3.4786E-05	4.8719E-07

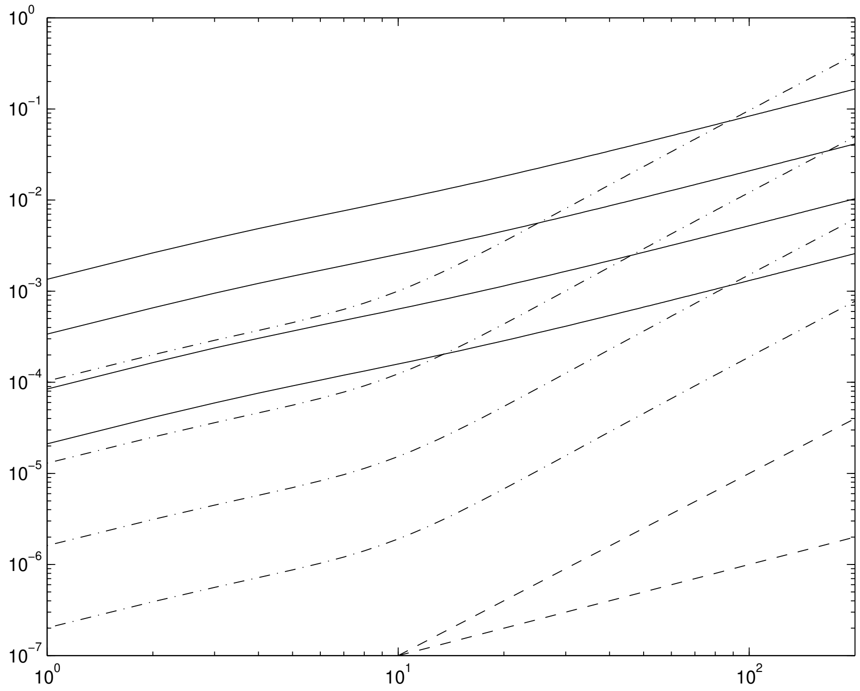

Figure 1: L^2-error against t. Solid line: [ICM]; dashed line: [NCM]. The time steps are $\Delta t = 1/20, 1/40, 1/80, 1/160$. The broken lines at the bottom show the slopes for linear and quadratic growth in time.

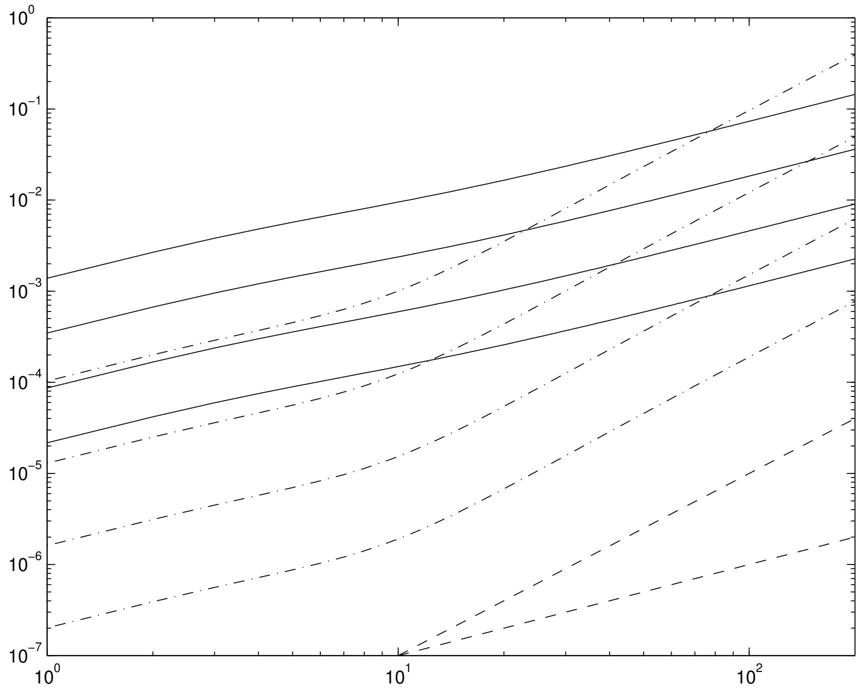

Figure 2: L^2-error against t. Solid line: [HCM]; dashed line: [NCM]. $\Delta t = 1/20, 1/40, 1/80, 1/160$. The broken lines at the bottom show the slopes for linear and quadratic growth in time.

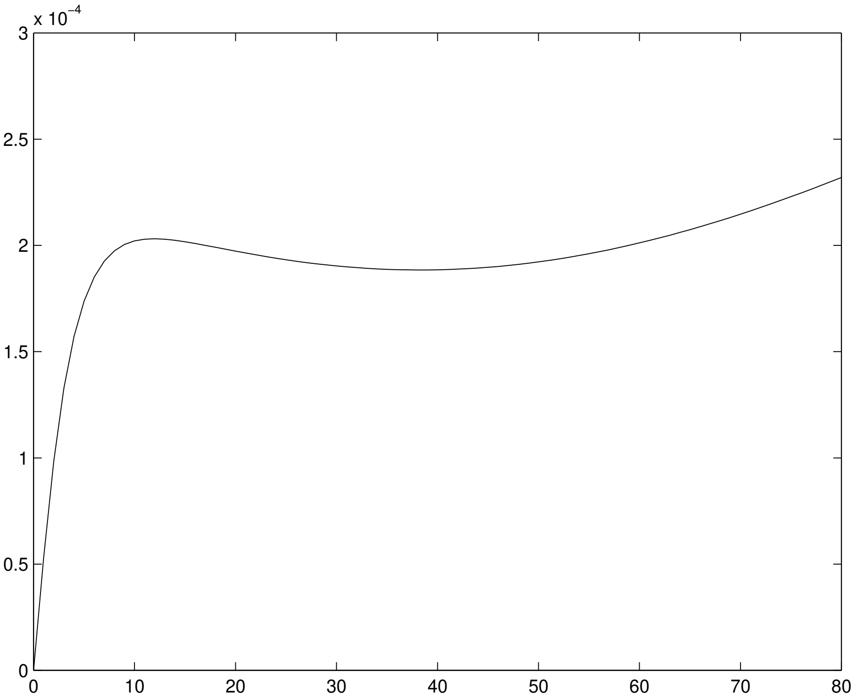

Figure 3: L^2-error with respect to the modified solitary wave against t. [HCM] with $\Delta t = 1/80$.

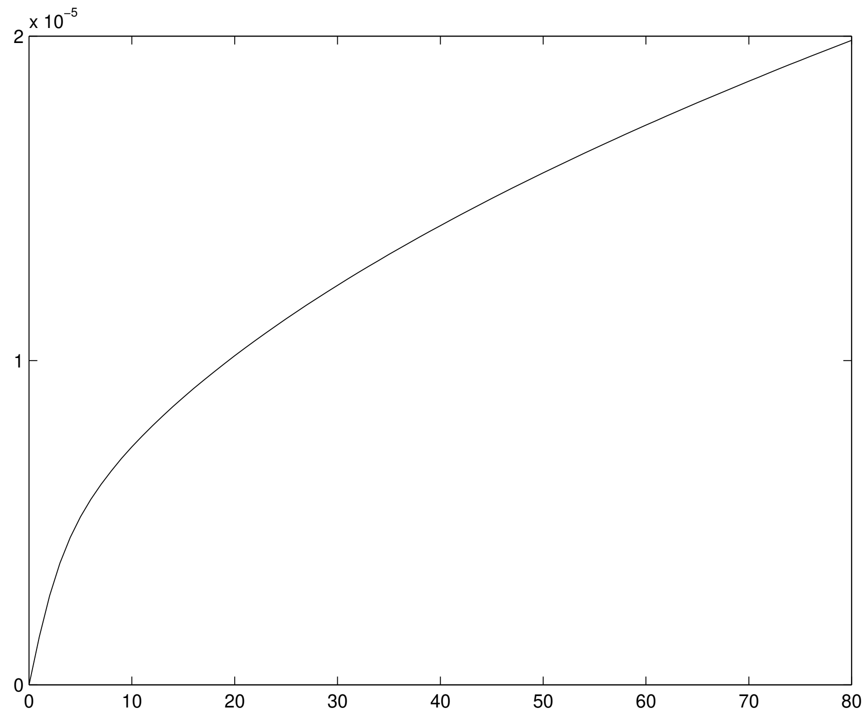

Figure 4: L^2-error with respect to the modified solitary wave against t. [NCM] with $\Delta t = 1/80$.

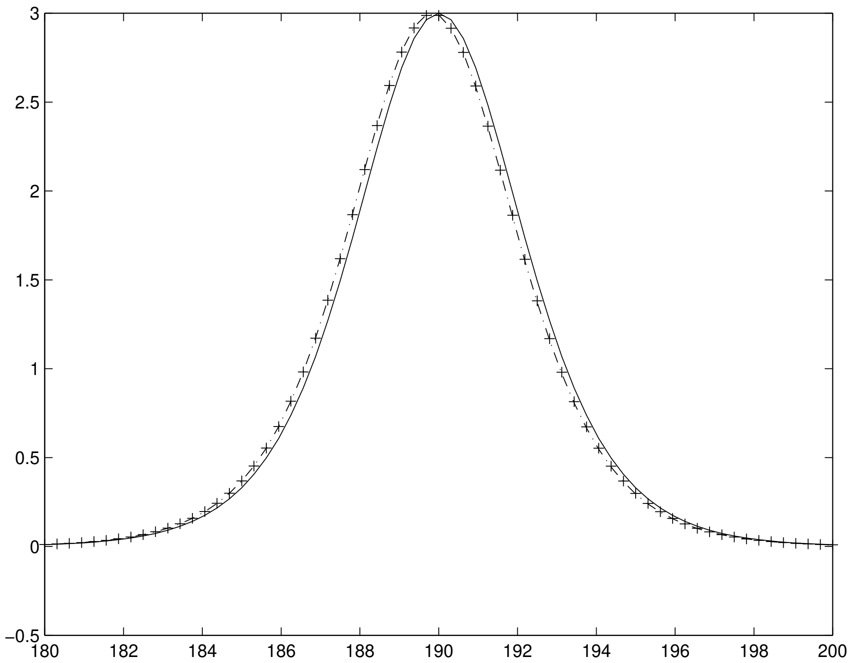

Figure 5: [HCM] with $\Delta t = 1/20$ at $t = 100$. Original solitary wave (solid line), modified wave (dashed line) and numerical solution (crosses).

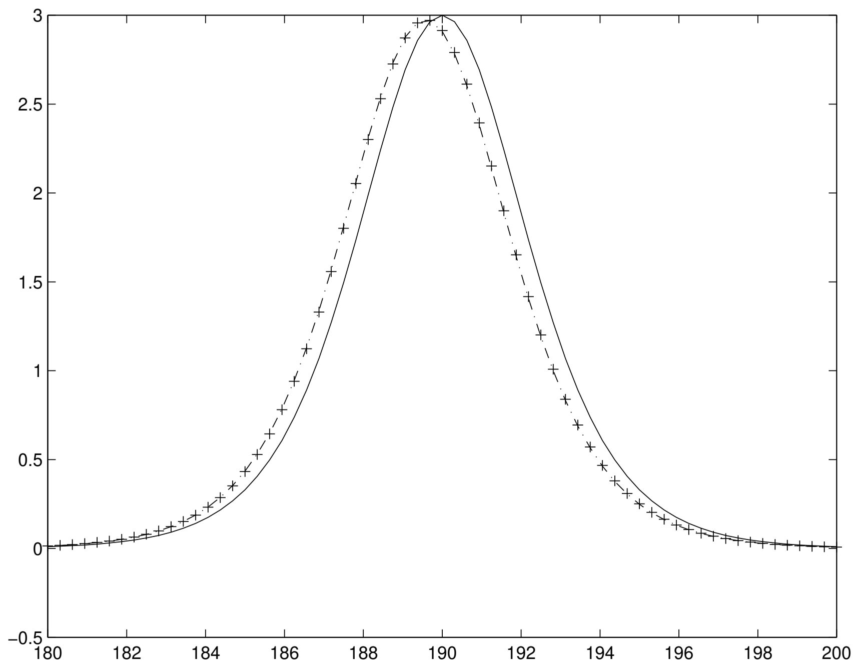

Figure 6: [NCM] with $\Delta t = 1/20$ at $t = 100$. Original solitary wave (solid line), modified wave (dashed line) and numerical solution (crosses).

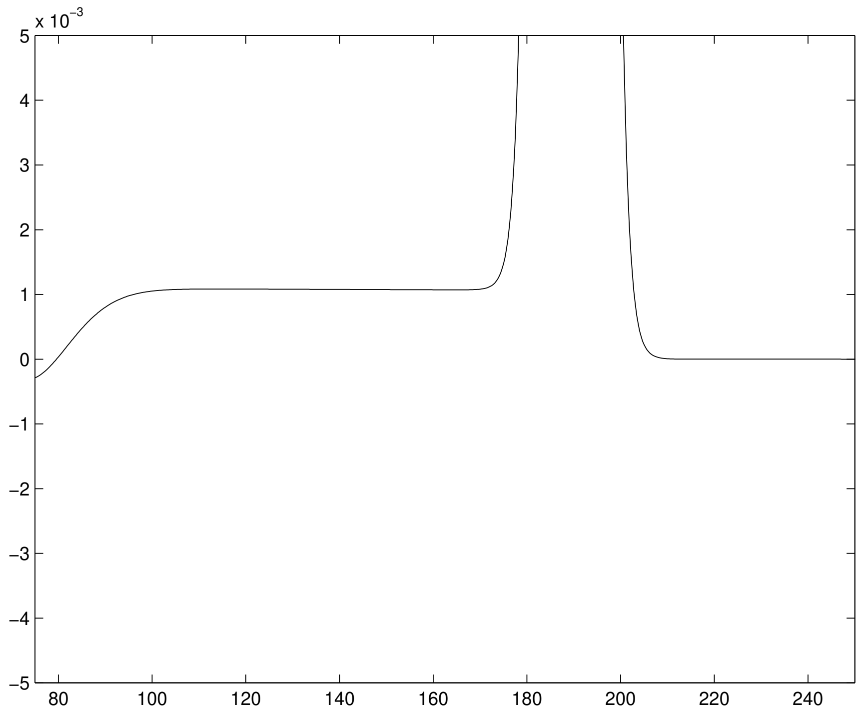

Figure 7: [NCM] with $\Delta t = 1/20$ at $t = 100$. Numerical solution with magnified vertical scale.

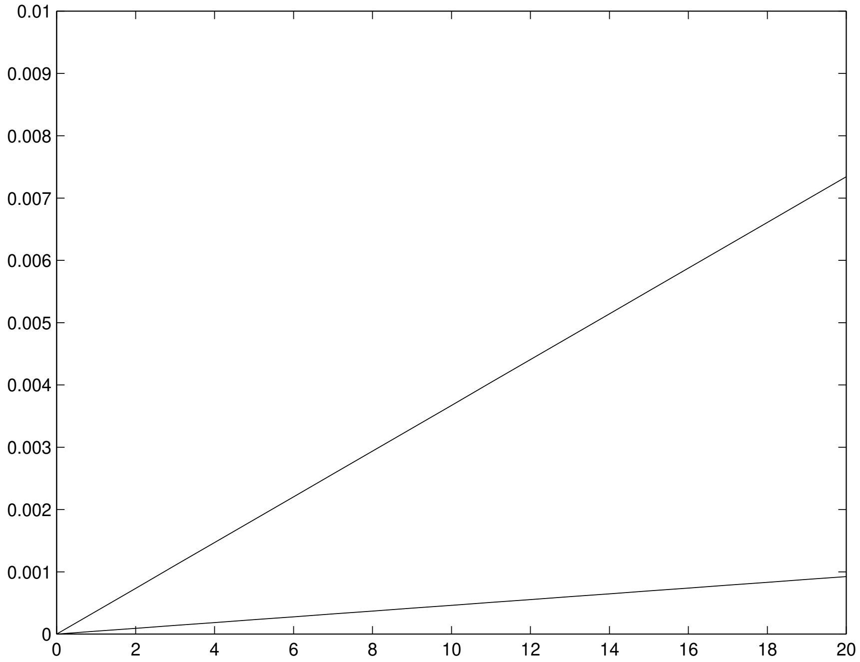

Figure 8: Energy error against t. [NCM] with $\Delta t = 1/20, 1/40$.

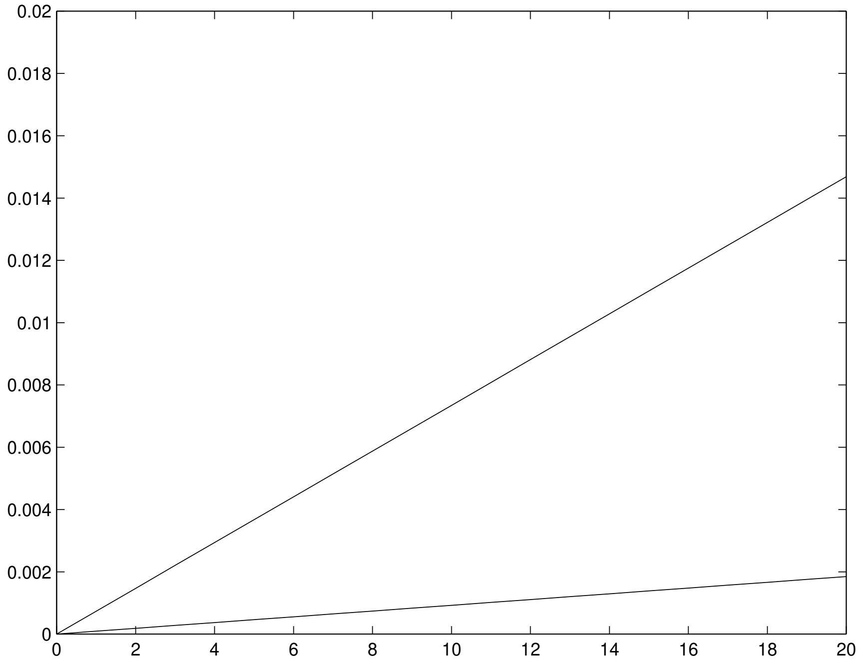

Figure 9: Energy error against t. [NCM] with $\Delta t = 1/20, 1/40$.

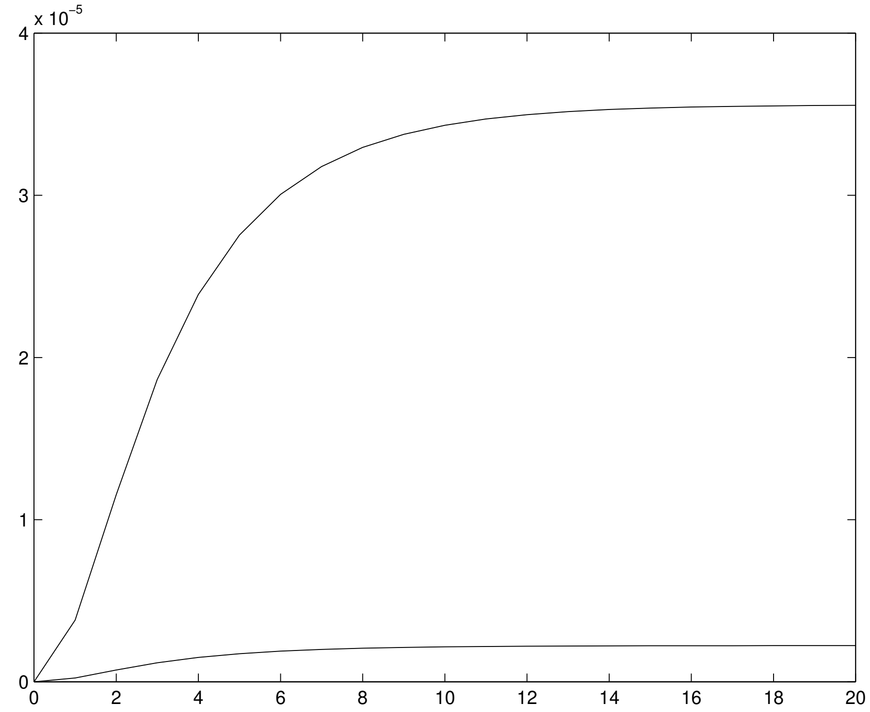

Figure 10: Momentum error against t. [HCM] with $\Delta t = 1/10, 1/20$.